

Adsorption behaviors of iodide anion on silver loaded macroporous silicas*

WU Hao (吴昊), WU Yan (吴艳),[†] CHEN Zi (陈梓), and WEI Yue-Zhou (韦悦周)

School of Nuclear Science and Engineering, Shanghai Jiao Tong University, Shanghai 200240, China

(Received July 31, 2014; accepted in revised form October 13, 2014; published online June 20, 2015)

A macroporous silica-based silver loaded adsorbent was synthesized by grafting the silver complexes of thiourea ($\text{Ag}(\text{tu})_3\text{NO}_3$) into a silica-based copolymer support ($\text{SiO}_2\text{-P}$). The adsorbent was used to uptake iodide anions (I^-) by batch and column techniques. The kinetic and saturated adsorption experiments were carried out by varying the shaking times and initial concentration of I^- . Experimental results shown that the kinetic adsorption of I^- was controlled by a pseudo second order model and the saturated adsorption of I^- was controlled by the chemisorption mechanism, which followed a Langmuir adsorption equation. The breakthrough curve of I^- had a S-shaped profile. The column efficiency was estimated to be over 90%.

Keywords: Iodide anion, Silver complexes of thiourea, Grafting, Macroporous silica-based support, Radioactive contaminated wastewater

DOI: [10.13538/j.1001-8042/nst.26.030301](https://doi.org/10.13538/j.1001-8042/nst.26.030301)

I. INTRODUCTION

Large amounts of radioactive contaminated wastewater (RCW) were generated from the nuclear accident at Fukushima NPP-1 in Japan. The RCW is reactor cooling water collected after contact with damaged nuclear fuel debris, so the main radionuclides are waste-soluble Cs (^{134}Cs , ^{137}Cs), Sr (^{90}Sr), and I (^{131}I , ^{129}I) [1]. With a half-life of 1.7×10^7 years, ^{129}I is a primary long-term risk driver in shallow land disposal facilities. ^{131}I would be an acute contaminant because of its short half-life of 8.05 days and high specific activity [2]. Releasing the untreated iodine contaminants into the environment would pollute the soil, air, and groundwater, resulting in long-term radioecological risk.

Aqueous iodine exists primarily as an iodide anion (I^-) and iodate anion (IO_3^-), depending on the redox conditions and pH. At low to neutral pH and positive redox potentials, the iodide anion is the dominant species in a solution environment [3]. The Fukushima RCW contains various co-existent components from sea water (saline elements), corrosion products, and ground-water. Its pH ranges from 7–8 [4]. In previous works, various methods have been developed to remove or adsorb iodide anion from aqueous solutions [5–7]. Common natural porous materials, such as alumina and hydrotalcite can absorb iodide anions through surface physical adsorption or ion exchange with an active group of the adsorbent materials [8]. However, the presence of the coexisting chloride anion in RCW can compete against iodide anion and render the natural materials without adsorption selectivity for iodide anions. Inorganic anion exchangers, such as $\text{BiPbO}_2(\text{NO}_3)$ were also reported to adsorb iodide anions [9]. But such inorganic anion exchangers are usually not easy to prepare and sometimes its toxicity is also a problem. The cuprous (Cu^+)-containing compounds react with iodide anions to form

cuprous iodide through the participation of hydrogen anions, this adsorption process is very sensitive to the pH of the solution, so the adsorption amount is rather low in neutral and slightly acidic solutions [10]. Recently, the silver adsorbents were investigated. The adsorption mechanism mainly related to the strong chemical interaction between silver and iodide anions, and the adsorbents have good selectivity. However, the leakage of the impregnated materials could result in the lowering of the adsorbed amount [11].

In this work, we attempted to synthesize a macroporous silica-based silver loaded adsorbent ($\text{Ag}(\text{tu})_3\text{NO}_3/\text{SiO}_2\text{-P}$) by grafting the silver complexes of thiourea ($\text{Ag}(\text{tu})_3\text{NO}_3$) into a silica-based copolymer support ($\text{SiO}_2\text{-P}$) for adsorbing iodide anions. The $\text{SiO}_2\text{-P}$ support is a kind of inorganic macroporous material, which was prepared by impregnating the copolymer inside the macroporous SiO_2 substrate [12]. Grafting the $\text{Ag}(\text{tu})_3\text{NO}_3$ into $\text{SiO}_2\text{-P}$ has a number of advantages, such as mechanical strength, strong acid, chemical stability, radiation resistance, and the ease of solid-liquid separation. Compared to the reported iodide adsorbents, the synthesized $\text{Ag}(\text{tu})_3\text{NO}_3/\text{SiO}_2\text{-P}$ is easy to prepare and can avoid silver leaching during adsorption. The adsorption kinetics, mechanisms, and dynamic adsorption behavior of iodide anions for $\text{Ag}(\text{tu})_3\text{NO}_3/\text{SiO}_2\text{-P}$ were investigated.

II. EXPERIMENTAL

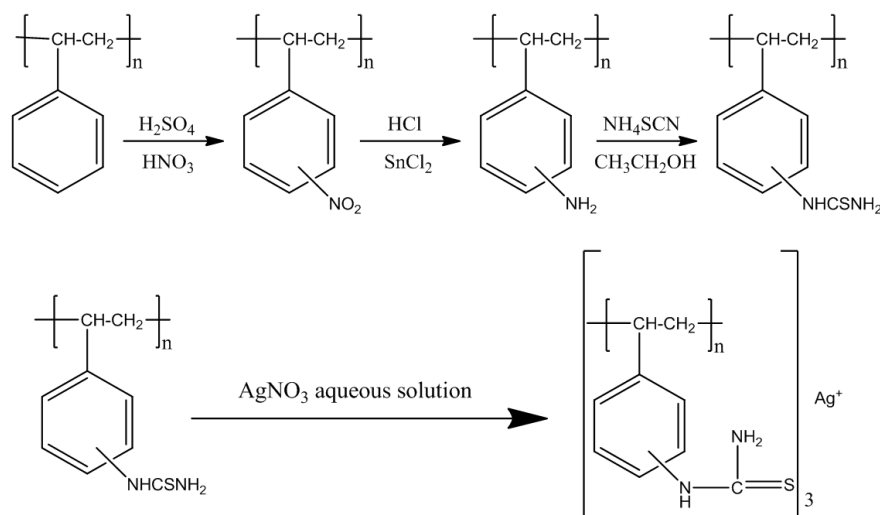
A. Materials

The reagents used in the experiments, such as Sulfuric acid (98%), Nitric acid (65%), hydrochloric acid (37%), Ethanol, Tin(II) chloride dehydrate, Ammonium thiocyanate, and Silver nitrate, are analytical grade or better.

The $\text{SiO}_2\text{-P}$ was synthesized based on a known method [13]. For simplicity, “P” in the $\text{SiO}_2\text{-P}$ particles was abbreviated as styrene-divinylbenzene (SDB) copolymer, which was immobilized inside the macroporous SiO_2 substrate through a polymerization reaction.

* Supported by National Natural Science Foundation of China (Nos. 21261140335 and 91126006) and the Scientific Research Foundation for Youth Scholars of Shanghai Jiao Tong University (No. AF0200003)

[†] Corresponding author, wu_yan@sjtu.edu.cn

Fig. 1. The synthesis procedures of $\text{Ag}(\text{tu})_3\text{NO}_3/\text{SiO}_2\text{-P}$.

B. Preparation of $\text{Ag}(\text{tu})_3\text{NO}_3/\text{SiO}_2\text{-P}$

The synthesis procedures of $\text{Ag}(\text{tu})_3\text{NO}_3/\text{SiO}_2\text{-P}$ were performed as follows:

- (1) $\text{SiO}_2\text{-P-NO}_2$ was prepared by nitration of the copolymer in $\text{SiO}_2\text{-P}$. $\text{SiO}_2\text{-P}$ was mixed with nitric acid (65%) and sulfuric acid (98%) in a water bath at 50°C for 3 h.
- (2) $\text{SiO}_2\text{-P-NO}_2$ was reduced to $\text{SiO}_2\text{-P-NH}_2$ in the presence of stannous chloride, hydrochloric acid (37%), and Ethanol in a water bath at 60°C for 12 h.
- (3) $\text{SiO}_2\text{-P-tu}$ was prepared by mixing $\text{SiO}_2\text{-P-NH}_2$, Ethanol, and Ammonium thiocyanate into a flask with water bath heating under 70°C , stirring for 12 h, filtering and drying under 50°C .
- (4) $\text{Ag}(\text{tu})_3\text{NO}_3/\text{SiO}_2\text{-P}$ was prepared by mixing an $\text{SiO}_2\text{-P-tu}$ and silver nitrate solution into a flask, stirring for 12 h, and filtering and drying under 50°C . The synthesis procedures are shown in Fig. 1. Many of the diverse structural types of $\text{Ag}(\text{I})/(x)\text{tu}$ ($x=1\sim n$) complexes have been reported. It was claimed that the $\text{Ag}(\text{I})/(3)\text{tu}$ complexes were the most common types [14–17].

C. Characterization

SEM analysis (Nova NanoSEM NPE218) was carried out to study the surface morphology of $\text{Ag}(\text{tu})_3\text{NO}_3/\text{SiO}_2\text{-P}$. The thermal stability of $\text{SiO}_2\text{-P}$ and $\text{Ag}(\text{tu})_3\text{NO}_3/\text{SiO}_2\text{-P}$ were evaluated. The analyses were performed by TG-DTA equipment (Shimadzu DTG-60) with a $10^\circ\text{C}/\text{min}$ constant heating rate from 25°C to 800°C . The FT-IR spectrum of the $\text{Ag}(\text{tu})_3\text{NO}_3/\text{SiO}_2\text{-P}$ was recorded in the range of $4000\text{--}500\text{ cm}^{-1}$ using the IRAffinity-1 FT-IR spectrometer.

D. The Static Experiments

The static experiment adsorption behavior of tested iodide anions on the adsorbent was examined by batch experiments using $\text{Ag}(\text{tu})_3\text{NO}_3/\text{SiO}_2\text{-P}$. An aqueous phase (5 mL), containing varying iodide anion concentrations, was equilibrated with 0.1 g adsorbents in stopper glass tubes in a thermo state water bath (Tokyo RIKAKIKA Co., Ltd.) at room temperature. The concentration of the tested iodide anions before and after adsorption was measured by ICP-AES (Shimadzu 7510). The adsorption capacity at equilibrium (Q_{eq}) can be calculated using the following formula

$$Q_{\text{eq}} = \frac{V}{m} \times (C_0 - C_e), \quad (1)$$

where C_0 and C_e are the initial and equilibrium concentrations of the iodide anions, m is the weight of the adsorbent, and V is the volume of the aqueous phase.

E. Column operation

The $\text{Ag}(\text{tu})_3\text{NO}_3/\text{SiO}_2\text{-P}$ (4.05 g) was densely packed into a glass column (10 mm in diameter, 200 mm long) with a thermo jacket set at $(25 \pm 1)^\circ\text{C}$, shown in Fig. 2. A breakthrough of iodide anions was tested at a feed solution of 1 mM NaI and the flow rate was controlled to $0.5\text{ cm}^3/\text{min}$.

III. RESULTS AND DISCUSSION

A. SEM

The SEM micrographs of $\text{Ag}(\text{tu})_3\text{NO}_3/\text{SiO}_2\text{-P}$ are shown in Fig. 3. Obvious spherical and porous particles were obtained. The practical size of $\text{Ag}(\text{tu})_3\text{NO}_3/\text{SiO}_2\text{-P}$ was estimated to be

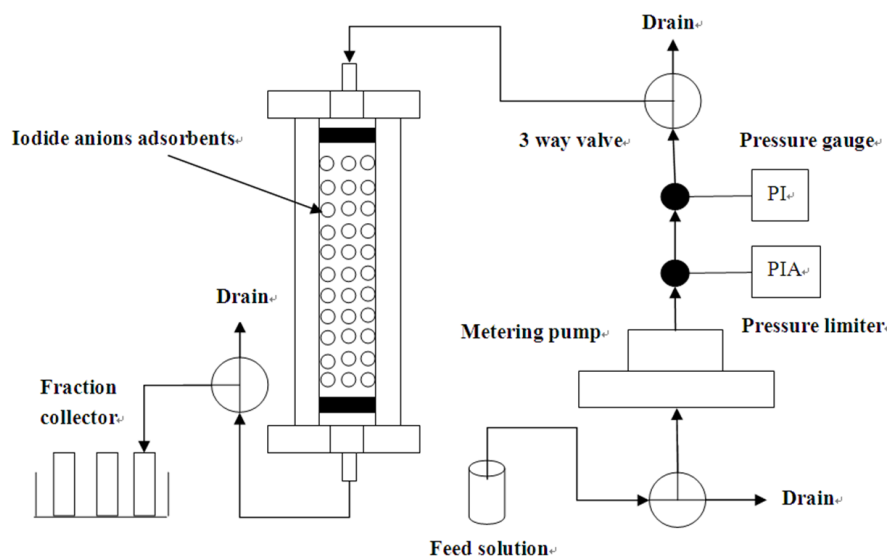


Fig. 2. Apparatus for the column experiments.

50 μm in diameter. From the smooth surface, it is found that the active ingredients were all impregnated inside the $\text{SiO}_2\text{-P}$.

B. TG-DTA

The results of TG and DTA for $\text{SiO}_2\text{-P}$ are shown in Fig. 4. It indicates two different weight loss ranges: 280–350 $^\circ\text{C}$ and 350–550 $^\circ\text{C}$. The first and second weight losses were due to the thermal desorption of the SDB copolymer [18]. The overall weight loss of $\text{SiO}_2\text{-P}$ was estimated to be 15%, indicating that 15 wt.% SDB was impregnated inside the SiO_2 substrate and the content of SiO_2 was calculated to be 85 wt.%.

The results of TG and DTA for $\text{Ag}(\text{tu})_3\text{NO}_3/\text{SiO}_2\text{-P}$ are shown in Fig. 5. It indicates three different weight loss ranges: the first and second weight losses denoted the burning of the SDB polymer, similar to those of Fig. 4. The third weight loss (400–550 $^\circ\text{C}$) was interpreted as the thermal decomposition of the silver complex of thiourea. The corresponding endothermic peak around 540 $^\circ\text{C}$ was also observed.

Thus, the content of the silver complex of thiourea grafted onto the copolymer was estimated to be 12%.

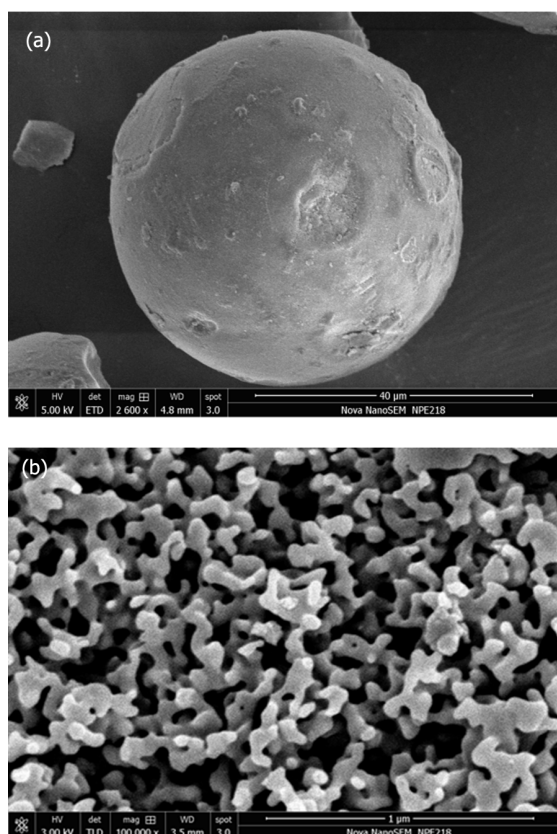
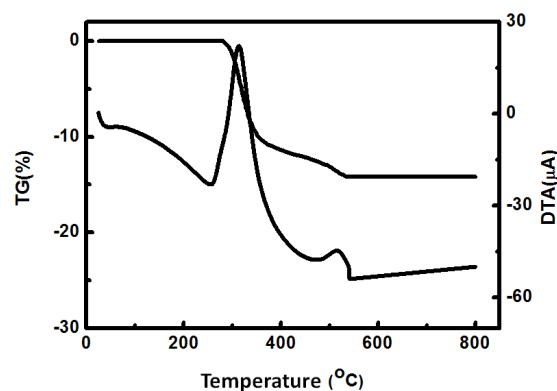
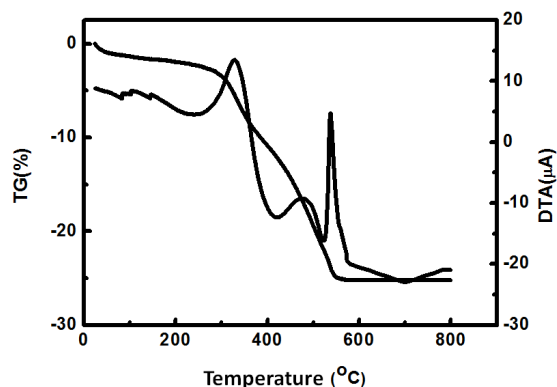
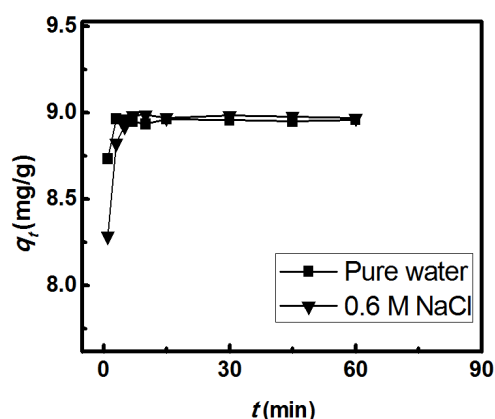


Fig. 3. SEM image of $\text{Ag}(\text{tu})_3\text{NO}_3/\text{SiO}_2\text{-P}$. (a) Surface micrograph of $\text{Ag}(\text{tu})_3\text{NO}_3/\text{SiO}_2\text{-P}$; (b) Inner micrograph of $\text{Ag}(\text{tu})_3\text{NO}_3/\text{SiO}_2\text{-P}$.

Fig. 4. TG-DTA curves of $\text{SiO}_2\text{-P}$.

Fig. 5. TG-DTA curves of $\text{Ag}(\text{tu})_3\text{NO}_3/\text{SiO}_2\text{-P}$.Fig. 6. The equilibrium time on the uptake of I^- , $V/m = 50 \text{ cm}^3/\text{g}$, $[\text{I}^-] = 200 \text{ ppm}$, 25°C .

C. Kinetic adsorption studies

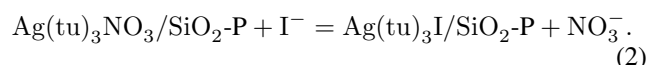
In this experiment, the effect of the contact time on the adsorption of the iodide anions by $\text{Ag}(\text{tu})_3\text{NO}_3/\text{SiO}_2\text{-P}$ was studied. To find out the relationship between the time of adsorption (t) and the amount adsorbed at a time of $t(q_t)$ are plotted and shown in Fig. 6.

D. FT-IR studies

The FT-IR spectrum of the $\text{Ag}(\text{tu})_3\text{NO}_3/\text{SiO}_2\text{-P}$ is shown in Fig. 7. Since the $\text{Ag}(\text{tu})_3\text{NO}_3$ was grafted into the holes of $\text{SiO}_2\text{-P}$, the FT-IR spectrum of the $\text{Ag}(\text{tu})_3\text{NO}_3/\text{SiO}_2\text{-P}$ shown in Fig. 7(a) was mainly dominated by the Si—O groups. In order to observe other chemical bonds clearly, partial enlarged details are shown in Figs. 7(b)–7(d). The sharp band observed at 1080 cm^{-1} in Fig. 7(a) was due to asymmetric vibrations of Si—O—Si. In addition, the band observed at 789 cm^{-1} was attributed to the symmetric stretching vibration peak of the Si—O bond [19]. After nitration, the IR spectrum of the $\text{SiO}_2\text{-P}$ showed the peaks at 1518 cm^{-1} and 1350 cm^{-1} , corresponding to N—O asymmetric and symmetric stretches, respectively. The asymmetric and symmetric vibrations

of the NH_2 groups were positioned between 3231 cm^{-1} and 3178 cm^{-1} , as shown in Figs. 7(d) [20]. The little shoulder observed at 1560 cm^{-1} in Fig. 7(c) was due to $\nu(\text{C}=\text{S})$, indicating the co-ordination of the C=S group to the Ag atom in the complex. In addition, the band observed at 768 cm^{-1} was assigned to the bending vibration of the C=S group. This also supported the co-ordination of the C=S group to the Ag atom in the complex [21, 22].

The adsorption equilibrium of iodide anions (I^-) on $\text{Ag}(\text{tu})_3\text{NO}_3/\text{SiO}_2\text{-P}$ was attained within 10 min in pure water. The adsorbed amount of I^- on $\text{Ag}(\text{tu})_3\text{NO}_3/\text{SiO}_2\text{-P}$ was 8.89 mg/g (Fig. 6). In 0.6 M NaCl solution (simulated seawater), it was observed that the equilibrium time of adsorption on $\text{Ag}(\text{tu})_3\text{NO}_3/\text{SiO}_2\text{-P}$ was similar to that in pure water. The uptake of I^- for the $\text{Ag}(\text{tu})_3\text{NO}_3/\text{SiO}_2\text{-P}$ adsorbent was governed by the following ion-exchange reactions [23]



The ability of the thiourea(tu) functional group to form a stable adduct with silver is well established [16]. $\text{Ag}(\text{tu})_3^+$ is different from Ag^+ , even in the NaCl solution, because the $\text{Ag}(\text{tu})_3^+$ will not react with Cl^- [24, 25]. Therefore, the $\text{Ag}(\text{tu})_3\text{NO}_3/\text{SiO}_2\text{-P}$ is effective for removing the I^- from the seawater.

In order to investigate the mechanism of adsorption and determine the rate-controlling step, the following kinetic model is used to test the experimental data.

The pseudo second-order kinetic model is represented by the following equation:

$$\frac{dq_t}{dt} = K_2 \times (Q_{\text{eq}} - q_t)^2 \quad (3)$$

Integrating Eq. (3) with the boundary conditions of (1) at $t = 0$ and $q_t = 0$ and (2) at $t = t$ and $q_t = q_t$ results in the following equation:

$$\frac{t}{q_t} = \frac{1}{K_2 Q_{\text{eq}}^2} + \frac{t}{Q_{\text{eq}}} \quad (4)$$

where K_2 ($\text{mg}/(\text{g min})$) is the adsorption rate constant for pseudo second-order kinetics, q_t (mg/g) is the amount of iodide anions adsorbed at time t , and Q_{eq} (mg/g) is the amount of iodide anions adsorbed at equilibrium [26].

The fit lines are shown in Fig. 8. It shows that the rate constants Q_{eq} and the regression values for pseudo second-order kinetics are greater than 0.99, indicating that the adsorption system belongs to the second-order kinetics model. The Q_{eq} and K_2 can be determined from a plot of t/q_t against t . The calculated values are summarized in Table 1. It shows that the calculated Q_{eq} values agree with the experimental data. These results indicate that I^- adsorption was a rate controlled step, which was governed by the chemisorption process.

E. Adsorption Isotherms

The Langmuir and Freundlich isotherm models were studied for the adsorption mechanism of iodide anions (I^-)

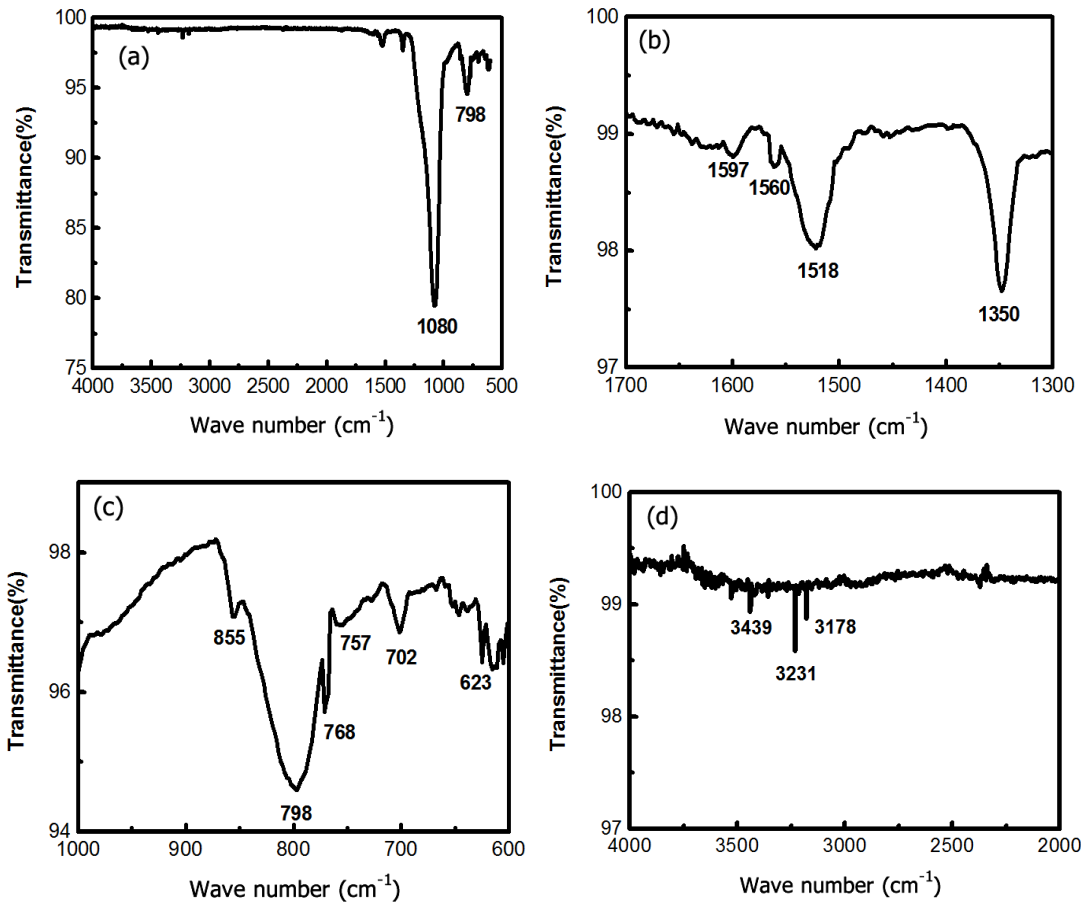


Fig. 7. FT-IR curves of $\text{Ag}(\text{tu})_3\text{NO}_3/\text{SiO}_2\text{-P}$.

TABLE 1. Kinetic constants for the adsorption of iodide anion ($T = 25^\circ\text{C}$)

Kinetic model	Parameter	Pure water	0.6 M NaCl
Pseudo second-order	Q_{eq} (mg/g)	8.96	8.98
	K_2 (mg/(g min))	12.45	4.42
	R^2	0.9999	0.9988

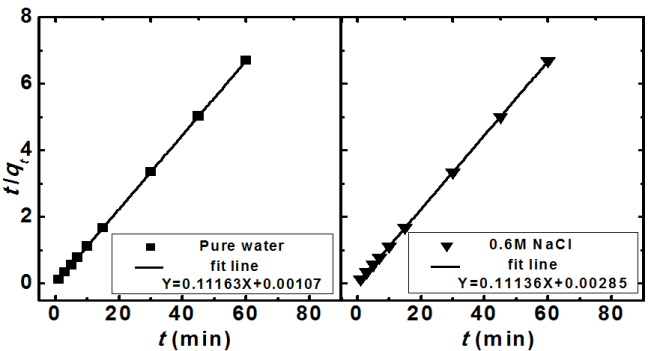


Fig. 8. Pseudo second-order kinetic fit for I^- adsorption, $V/m = 50 \text{ cm}^3/\text{g}$, $[\text{I}^-] = 200 \text{ ppm}$, 25°C .

on $\text{Ag}(\text{tu})_3\text{NO}_3/\text{SiO}_2\text{-P}$. The isotherm parameters were determined using Origin software, which showed the plots of C_{eq} versus Q_{eq} for different isotherms.

1. Langmuir isotherm

The Langmuir isotherm is given by the following equation:

$$\frac{C_{\text{eq}}}{Q_{\text{eq}}} = \frac{1}{Q_{\text{max}}} C_{\text{eq}} + \frac{1}{K_L Q_{\text{max}}}, \quad (5)$$

where Q_{max} is the maximum monolayer adsorption capacity (mg/g), K_L is the equilibrium constant related to free energy (L/mg), C_{eq} is the concentration of the iodide anions at equilibrium (mg/L), and Q_{eq} is the amount of iodide anions adsorbed at equilibrium (mg/g) [27].

2. Freundlich isotherm

The Freundlich isotherm applies to multilayer adsorption and adsorption on a heterogeneous surface. It is given by the following equation

$$\lg Q_{\text{eq}} = \frac{1}{n} \lg C_{\text{eq}} + \lg K_F, \quad (6)$$

where Q_{eq} is the amount of iodide anions adsorbed at equilibrium (mg/g), C_{eq} is the concentration of the iodide anions at equilibrium (mg/L), n is the measure of deviation from linearity of adsorption, and K_F is the adsorption capacity related to a multilayer (mg/g).

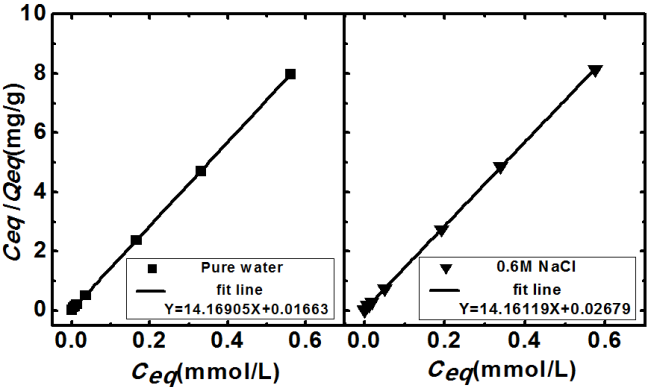


Fig. 9. Langmuir fit for I^- adsorption, $V/m = 50 \text{ cm}^3/\text{g}$, $[I^-] = 200 \text{ ppm}$, 25°C .

TABLE 2. Isotherm constants for adsorption of I^- ($T = 25^\circ\text{C}$)

Adsorption model	Parameter	Pure water	0.6 M NaCl
Langmuir isotherm	$Q_{\max}(\text{mg/g})$	8.94	8.96
	K_L	6.71	4.16
	R^2	0.9999	0.9989
Freundlich isotherm	n	5.29	4.98
	K_F	0.04	0.04
	R^2	0.6413	0.6561

The linear plot of C_{eq}/Q_{eq} vs. C_{eq} shows that adsorption follows a Langmuir isotherm (Fig. 9). The applicability of the Langmuir isotherm suggests monolayer coverage of iodide anions on the surface of $\text{Ag}(\text{tu})_3\text{NO}_3/\text{SiO}_2\text{-P}$. The values of Q_{\max} and K_L were calculated from the slope and intercept of the linear plots and presented in Table 2. It shows that the adsorption Q_{\max} value for $\text{Ag}(\text{tu})_3\text{NO}_3/\text{SiO}_2\text{-P}$ in 0.6 M NaCl was calculated to be 8.96 mg/g, similar to that in pure water. On the other hand, the fitted Freundlich plots show a low R^2 value around 0.6 (Fig. 10), indicating the inapplicability of the Freundlich isotherm.

F. The column experiments

The performance of the fixed-bed adsorption is complemented by the dynamic column studies, which can be deduced from the concept of a breakthrough curve. The breakthrough curve is usually expressed in terms of inlet concentration (C_0) and outlet concentration (C), and is defined as the ratio of outlet concentration to inlet concentration (C/C_0) as a function of effluent for a given bed height [16].

A breakthrough of I^- was tested at a feed solution of 1 mM NaI and at a high flow rate of $0.5 \text{ cm}^3/\text{min}$. Figure 11 illustrates the breakthrough curve of I^- , which has a S-shaped

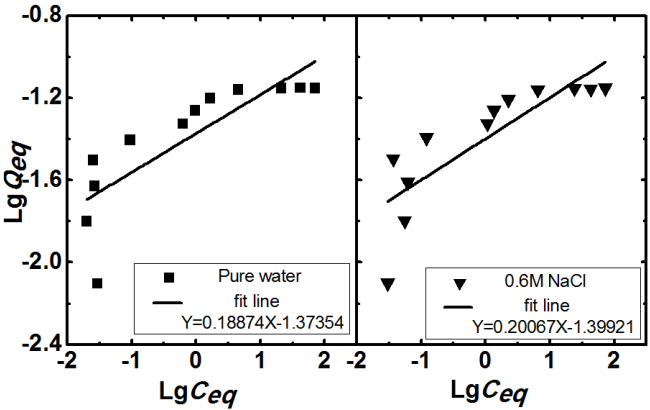


Fig. 10. Freundlich fit for I^- adsorption, $V/m = 50 \text{ cm}^3/\text{g}$, 25°C .

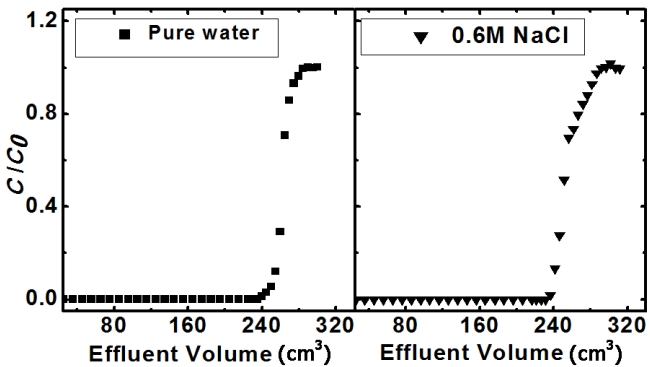


Fig. 11. Breakthrough curves of I^- , $\text{Ag}(\text{tu})_3\text{NO}_3/\text{SiO}_2\text{-P}$: 4.05 g; feed: 1 mM $[I^-]$; flow rate: $0.5 \text{ cm}^3/\text{min}$; $T = 25^\circ\text{C}$.

profile and a steep slope, suggesting no dislodgement of $\text{Ag}(\text{tu})_3\text{NO}_3$ from the matrix of $\text{SiO}_2\text{-P}$. The break point of 5% breakthrough was estimated to be 235 and 231 cm^3 and the column took approximately 284 and 286 cm^3 before being completely exhausted with I^- . The breakthrough capacity (B.T. Cap.) and the total capacity (T. Cap.) were calculated to be 7.24 mg/g and 7.87 mg/g, respectively in 0.6 M NaCl solution, resulting in a relatively high column efficiency (B.T. Cap./T. Cap.) of 91.9%. The adsorption behavior of I^- on $\text{Ag}(\text{tu})_3\text{NO}_3/\text{SiO}_2\text{-P}$ in pure water was close to that in 0.6 M NaCl, indicating that the adsorption of I^- was not affected by the presence of the Cl^- anions in seawater. The column packed with $\text{Ag}(\text{tu})_3\text{NO}_3/\text{SiO}_2\text{-P}$ was thus effective for removing I^- from radioactive contaminated wastewater, even containing highly concentrated NaCl.

IV. CONCLUSION

The macroporous silica-based $\text{Ag}(\text{tu})_3\text{NO}_3/\text{SiO}_2\text{-P}$ resin was prepared by grafting $\text{Ag}(\text{tu})_3\text{NO}_3$ onto an SiO_2 support. The uptake properties of I^- were investigated by a batch method and the adsorption behaviors of I^- were further studied by the column method in pure water and in 0.6 M NaCl solution.

The thermal stability of $\text{Ag}(\text{tu})_3\text{NO}_3/\text{SiO}_2\text{-P}$ indicated the adsorption ability of $\text{Ag}(\text{tu})_3\text{NO}_3/\text{SiO}_2\text{-P}$ can be maintained at temperatures up to 200 °C. The adsorption of I^- was fairly fast in both pure water and 0.6 M NaCl solution. The adsorption equilibrium can be attained within 10 min. The kinetic data was modeled successfully using the pseudo second-order kinetic model. The adsorption of I^- fit well with the Lang-

muir model and the correlation coefficient (R^2) was more than 0.99, suggesting a monolayer of adsorbent molecules on the surface of $\text{Ag}(\text{tu})_3\text{NO}_3/\text{SiO}_2\text{-P}$. The $\text{Ag}(\text{tu})_3\text{NO}_3/\text{SiO}_2\text{-P}$ effectively adsorbed iodide anions in the presence of 0.6 M NaCl in the column operation. From the results of this study, $\text{Ag}(\text{tu})_3\text{NO}_3/\text{SiO}_2\text{-P}$ is proposed to be an efficient adsorbent for the separation of iodide anions from radioactive waste water.

- [1] Sylvester P, Milner T and Jensen J. Radioactive liquid waste treatment at Fukushima Daiichi. *J Chem Technol Biot*, 2013, **88**: 1592–1596. DOI: [10.1002/jctb.4141](https://doi.org/10.1002/jctb.4141)
- [2] Hu Q H, Zhao P H, Moran J E, *et al.* Sorption and transport of iodine species in sediments from the Savannah River and Hanford Sites. *J Contam Hydrol*, 2005, **78**: 185–205. DOI: [10.1016/j.jconhyd.2005.05.007](https://doi.org/10.1016/j.jconhyd.2005.05.007)
- [3] Karanfil T, Moro E C and Serkiz S M. Development and testing of a silver chloride-impregnated activated carbon for aqueous removal and sequestration of iodide. *Environ Technol*, 2005, **26**: 1255–1262. DOI: [10.1080/09593332608618595](https://doi.org/10.1080/09593332608618595)
- [4] Sachse A, Merceille A, Barré Y, *et al.* Macroporous LTA-monomoliths for in-flow removal of radioactive strontium from aqueous effluents: Application to the case of Fukushima. *Microporous Mesoporous Mater*, 2012, **164**: 251–258. DOI: [10.1016/j.micromeso.2012.07.019](https://doi.org/10.1016/j.micromeso.2012.07.019)
- [5] Nagata T, Fukushi K and Takahashi Y. Prediction of iodide adsorption on oxides by surface complexation modeling with spectroscopic confirmation. *J Colloid Interf Sci*, 2009, **332**: 309–316. DOI: [10.1016/j.jcis.2008.12.037](https://doi.org/10.1016/j.jcis.2008.12.037)
- [6] Brown C F, Geiszler K N and Vickerman T S. Extraction and quantitative analysis of iodine in solid and solution matrixes. *Anal Chem*, 2005, **77**: 7062–7066. DOI: [10.1021/ac050972v](https://doi.org/10.1021/ac050972v)
- [7] Ensafi A A and Eskandari H. Efficient and selective extraction of iodide through a liquid membrane. *Microchem J*, 2001, **69**: 45–50. DOI: [10.1016/S0026-265X\(00\)00188-0](https://doi.org/10.1016/S0026-265X(00)00188-0)
- [8] Dai J L, Zhang M, Hu Q H, *et al.* Adsorption and desorption of iodine by various Chinese soils: II. Iodide and iodate. *Geoderma*, 2009, **153**: 130–135. DOI: [10.1016/j.geoderma.2009.07.020](https://doi.org/10.1016/j.geoderma.2009.07.020)
- [9] Kodama H and Kabay N. Reactivity of inorganic anion exchanger $\text{BiPbO}_2(\text{NO}_3)$ with fluoride ions in solution. *Solid State Ionics*, 2001, **141–142**: 603–607. DOI: [10.1016/S0167-2738\(01\)00775-5](https://doi.org/10.1016/S0167-2738(01)00775-5)
- [10] Lefèvre G, Walcarius A, Ehrhardt J J, *et al.* Sorption of iodide on cuprite (Cu_2O). *Langmuir*, 2000, **16**: 4519–4527. DOI: [10.1021/la9903999](https://doi.org/10.1021/la9903999)
- [11] Zhang H F, Gao X L, Guo T, *et al.* Adsorption of iodide ions on a calcium alginate-silver chloride composite adsorbent. *Colloid Surface A*, 2011, **386**: 166–171. DOI: [10.1016/j.colsurfa.2011.07.014](https://doi.org/10.1016/j.colsurfa.2011.07.014)
- [12] Wu Y, Kim S Y, Tozawa D, *et al.* Study on selective separation of cesium from high level liquid waste using a macroporous silica-based supramolecular recognition adsorbent. *J Radioanal Nucl Ch*, 2012, **293**: 13–20. DOI: [10.1007/s10967-012-1738-6](https://doi.org/10.1007/s10967-012-1738-6)
- [13] Wei Y Z, Kumagai M, Takashima Y, *et al.* Studies on the separation of minor actinides from high-level wastes by extraction chromatography using novel silica-based extraction resins. *Nucl Technol*, 2000, **132**: 413–423.
- [14] Bowmaker G A, Skelton B W and White A H. Structural and infrared spectroscopic studies of some novel mechanochemically accessed adducts of silver(I) oxoanion salts with thiourea. *Inorg Chem*, 2009, **48**: 3185–3197. DOI: [10.1021/ic802312j](https://doi.org/10.1021/ic802312j)
- [15] Pleyrier J and Cremers A. Stability of silver-thiourea complexes in montmorillonite clay. *J Chem Soc*, 1975, **71**: 256–264. DOI: [10.1039/F19757100256](https://doi.org/10.1039/F19757100256)
- [16] Ahmad S, Isab A A and Perzanowski H P. Silver(I) complexes of thiourea. *Transit Metal Chem*, 2002, **27**: 782–785. DOI: [10.1023/A:1020350023536](https://doi.org/10.1023/A:1020350023536)
- [17] Murthy D S R and Prasad P M. Leaching of gold and silver from Miller Process dross through non-cyanide leachants. *Hydrometallurgy*, 1996, **42**: 27–33. DOI: [10.1016/0304-386X\(95\)00049-M](https://doi.org/10.1016/0304-386X(95)00049-M)
- [18] Wu Y, Kim S Y, Tozawa D, *et al.* Equilibrium and kinetic studies of selective adsorption and separation for strontium using $\text{DtBuCH}_{18}\text{C}_6$ loaded resin. *J Nucl Sci Technol*, 2012, **49**: 320–327. DOI: [10.1080/00223131.2012.660022](https://doi.org/10.1080/00223131.2012.660022)
- [19] Mülle K, Foerstendorf H, Brendler V, *et al.* Sorption of Np(V) onto TiO_2 , SiO_2 , and ZnO : An in situ ATR FT-IR spectroscopic study. *Environ Sci Technol*, 2009, **43**: 7665–7670. DOI: [10.1021/es901256v](https://doi.org/10.1021/es901256v)
- [20] Lala N L, Deivaraj T C and Lee J Y. Auto-deposition of gold on chemically modified polystyrene beads. *Colloid Surface A*, 2005, **269**: 119–124. DOI: [10.1016/j.colsurfa.2005.06.073](https://doi.org/10.1016/j.colsurfa.2005.06.073)
- [21] Joseph G P, Rajarajan K, Vimalan M, *et al.* Spectroscopic, thermal and mechanical behavior of allylthiourea cadmium chloride single crystals. *Mater Res Bull*, 2007, **42**: 2040–2047. DOI: [10.1016/j.materresbull.2007.02.002](https://doi.org/10.1016/j.materresbull.2007.02.002)
- [22] Bowmaker G A, Skelton B W and White A H. Structural and infrared spectroscopic studies of some novel mechanochemically accessed adducts of silver(I) oxoanion salts with thiourea. *Inorg Chem*, 2009, **48**: 3185–3197. DOI: [10.1021/ic802312j](https://doi.org/10.1021/ic802312j)
- [23] El Aamrani F Z, Sastre A, Aguilar M, *et al.* Iodide-selective electrodes based on the silver(I) complex of a novel N-thiocarbamoylimine-dithioether derivative. *Anal Chim Acta*, 1996, **329**: 247–252. DOI: [10.1016/0003-2670\(96\)00115-8](https://doi.org/10.1016/0003-2670(96)00115-8)
- [24] Sandberg R G and Huiatt J L. Ferric chloride, thiourea and brine leach recovery of Ag, Au and Pb from complex sulfides. *JOM*, 1986, **38**: 18–22. DOI: [10.1007/BF03257810](https://doi.org/10.1007/BF03257810)
- [25] El Aamrani F Z, Garcia-Raurich J, Sastre A, *et al.* PVC membranes based on silver(I)-thiourea complexes. *Anal Chim Acta*, 1999, **402**: 129–135. DOI: [10.1016/S0003-2670\(99\)00562-0](https://doi.org/10.1016/S0003-2670(99)00562-0)
- [26] Senthilkumar T, Raghuraman R and Miranda L R. Parameter optimization of activated carbon production from *Agave sisalana* and *Punica granatum* peel: adsorbents for C.I. reactive orange 4 removal from aqueous solution. *Clean*, 2013, **41**: 797–807. DOI: [10.1002/clen.201100719](https://doi.org/10.1002/clen.201100719)
- [27] Jain R, Sharma P and Sikarwar S. Kinetics and isotherm analysis of Tropaeoline 000 adsorption onto unsaturated polyester resin (UPR): a non-carbon adsorbent. *Environ Sci Pollut R*, 2013, **20**: 1493–1502. DOI: [10.1007/s11356-012-0994-x](https://doi.org/10.1007/s11356-012-0994-x)